Photoinduced Electron Transfer between Cytochrome *c* Peroxidase and Yeast Cytochrome *c* Labeled at Cys 102 with (4-Bromomethyl-4′-methylbipyridine)[bis(bipyridine)]ruthenium^{2+} †

Lois Geren, Seung Hahm, Bill Durham,* and Francis Millett*
Department of Chemistry and Biochemistry, University of Arkansas, Fayetteville, Arkansas 72701
Received January 22, 1991; Revised Manuscript Received July 19, 1991

ABSTRACT: The synthesis of (4-bromomethyl-4′-methylbipyridine)[bis(bipyridine)]ruthenium(II) hexafluorophosphate is described. This new reagent was found to selectively label the single sulfhydryl group at Cys-102 on yeast iso-1-cytochrome *c* to form the (dimethylbipyridine-Cys-102-cytochrome *c*)[bis(bipyridine)]ruthenium derivative (Ru-102-cyt *c*). Excitation of Ru-102-cyt *c* with a short light flash resulted in formation of excited-state Ru(II*), which rapidly transferred an electron to the ferric heme group to form Fe(II). When the cytochrome *c* peroxidase compound I (CMPI) was present in the solution, electron transfer from photoreduced Fe(II) in Ru-102-cyt *c* to the radical site in CMPI was observed. At high ionic strength (100 mM sodium phosphate and 25 mM EDTA, pH 7), second-order kinetics were observed with a rate constant of $(7.5 \pm 0.7) \times 10^7$ M^{-1} s^{-1}. The second-order rate constant for native iso-1-cytochrome *c* was $(6.7 \pm 0.7) \times 10^7$ M^{-1} s^{-1} under these conditions. The second-order rate constant for electron transfer from Ru-102-cyt *c* to the radical site in CMPI increased as the ionic strength was decreased, reaching a value of $(4.8 \pm 0.5) \times 10^8$ M^{-1} s^{-1} in 40 mM EDTA, pH 7. At lower ionic strength, a complex was formed between Ru-102-cyt *c* and CMPI, and the rate for intracomplex electron transfer to the radical site was found to be greater than 50 000 s^{-1}. As a series of light flashes were used to titrate CMPI to CMPII, the reaction between Ru-102-cyt *c* Fe(II) and the Fe(IV) site in CMPII was observed. The intracomplex rate constant for this reaction was 250 ± 50 s^{-1} at low ionic strength (5 mM EDTA and 5 mM sodium phosphate, pH 7) and increased to 1000 ± 200 s^{-1} in 10 mM EDTA and 5 mM sodium phosphate. At still higher ionic strengths this reaction became second order, but it was slower than electron transfer to the radical site in CMPI under all conditions.

Biological electron transfer reactions between redox proteins play an essential role in many important biological processes. However, the measurement of the actual intracomplex electron transfer reaction remains a difficult problem, and only a few techniques have been utilized to study this process. The reaction between cytochrome *c* and cytochrome *c* peroxidase has been the focus of many of these techniques because of the detailed structural information available for each protein. The X-ray crystal structure of yeast cytochrome *c* peroxidase has been determined for the resting ferric form of the enzyme, CcP, (Finzel et al., 1984), the hydrogen peroxide oxidized form, CMPI (Edwards et al., 1987), and several mutant forms (Wang et al., 1990). A hypothetical structure for the 1:1 complex between cytochrome *c* peroxidase and cytochrome *c* has been proposed by using molecular modeling techniques (Poulos & Kraut, 1980).

The catalytic mechanism for cytochrome *c* peroxidase is very complex, as discussed recently by Kim et al. (1990). Hydrogen peroxide oxidizes ferric CcP to CMPI, which contains an oxyferryl heme Fe(IV) and a radical cation located on Trp 191 (Mauro et al., 1988; Sivaraja et al., 1989). CMPI is then sequentially reduced to CMPII and CcP in two one-electron steps involving ferrocytochrome *c*. Two forms of the singly oxidized state CMPII have been identified, CMPII(IV,R) containing the oxyferryl heme Fe(IV) and CMPII(III,R$^{\bullet+}$) containing the radical cation (Coulson et al, 1971; Ho et al., 1983). Summers and Erman (1988) reported that horse cytochrome *c* reduced the oxyferryl Fe(IV) site in CMPI with an intracomplex rate constant of 450 s^{-1} under stopped-flow conditions at low ionic strength. Hazzard et al. (1987, 1988a–c) utilized a flavin flash photolysis technique to study the intracomplex electron transfer reaction between yeast cytochrome *c* and CMPI. The rate constant increased from 250 s^{-1} at low ionic strength to 1460 s^{-1} at 260 mM ionic strength, suggesting that encounter complexes with more favorable geometries for electron transfer were formed at higher ionic strength. Wallin et al. (1991) have recently reported multiphasic intracomplex electron transfer from ferrocytochrome *c* to the zinc porphyrin cation of zinc cytochrome *c* peroxidase.

Scheme I

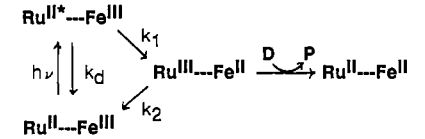

We have introduced a new technique to study intracomplex electron transfer that utilizes a substituted [tris(bipyridine)]ruthenium complex attached to one of the proteins (Pan et al., 1990). Pan et al. (1988) developed methods to prepare cytochrome *c* derivatives labeled at single lysine amino groups with [bis(bipyridine)](dicarboxybipyridine)ruthenium(II) [Ru(II)(bpy)$_2$(dcbpy)].[1] The Ru(II) group can be photoexcited to a metal-to-ligand charge transfer state, Ru(II*), which is a strong reducing agent and can rapidly transfer an electron to heme Fe(III) (Scheme I). The rate constants

† This work was supported by NIH Grants NIH GM20488 and RR07101.

[1] Abbreviations: bpy, 2,2′-bipyridine; dmbpy, 4,4′-dimethylbipyridine; Ru-102-cyt *c*, (bipyridine)$_2$(4,4′-dimethylbipyridine-Cys-102-cytochrome *c*)ruthenium(II); EDTA, ethylenediaminetetraacetic acid.

0006-2960/91/0430-9450$02.50/0

Scheme II

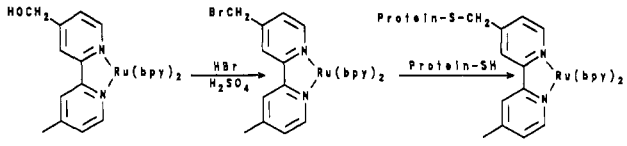

for this reaction ranged from 2×10^7 s^{-1} down to 10^5 s^{-1} for derivatives with ruthenium to heme separations ranging from 8 to 16 Å (Durham et al., 1989).

In the present paper we report the preparation of a new reagent, (4-bromomethyl-4′-methylbipyridine)[bis(bipyridine)]ruthenium,$^{2+}$ which specifically labels protein cysteine sulfhydryl groups (Scheme II). The purification problem is greatly simplified compared to the lysine reagent discussed above. The method also provides a route to attach ruthenium to proteins containing a cysteine residue introduced into a desired location by site-directed mutagenesis. The reagent has been used to label yeast iso-1-cytochrome *c* at the single sulfhydryl at cysteine 102 on the back side of the molecule opposite from the heme crevice. (The amino acid numbering system for tuna cytochrome *c* is used in the present paper.) The kinetics of the electron transfer reaction from Ru-102-cyt *c* to yeast cytochrome *c* peroxidase have been studied by photoexcitation of the ruthenium group.

Experimental Procedures

Materials. Bakers' yeast cytochrome *c* was purchased from Sigma Chemical Co. (type VIII-B) and was found to consist almost exclusively of iso-1-cytochrome *c*. Cytochrome *c* peroxidase was prepared from Red Star bakers' yeast by a modification of the method of Smith and Millett (1980) in which sodium phosphate buffers (pH 5) were used in place of the original sodium acetate buffers in the chromatographic steps. The enzyme was stored at −90 °C in phosphate buffers until use. It was rapidly oxidized by hydrogen peroxide and had the same visible spectra in each redox state as reported in the literature (Coulson et al., 1971). 4,4′-Dimethyl-2,2′-bipyridine was obtained from GFS Chemicals.

Preparation of [*Ru*(*bpy*)$_2$(*4-bromomethyl-4′-methylbipyridine*)](*PF*$_6$)$_2$: (*A*) *4-Formyl-4′-methylbipyridine.* 4,4′-Dimethyl-2,2′-bipyridine (4 g, 0.022 mol) was dissolved in 200 mL of 1,4-dioxane, selenium(IV) oxide (4 g, 0.036 mol) was added, and the solution was refluxed for 36 h [adopted from Furue et al. (1986) and Gosh and Spiro (1981)]. The yellow solution was vacuum-filtered to remove the black precipitate, and the dioxane was removed under reduced pressure. The solid was redissolved in chloroform, and the solution was filtered to remove excess selenium byproducts. The chloroform was then removed under reduced pressure. The chloroform suspension and filtration steps were repeated as needed to remove all of the selenium byproducts. Yield: 3.8 g, 0.020 mol (95%). ^{1}H NMR ($CDCl_3$): CH_3, 2.43; CHO, 10.18; aromatic, 7.15–8.93.

(*B*) *4-Hydroxymethyl-4′-methylbipyridine.* 4-Formyl-4′-methylbipyridine (3.8 g, 0.020 mol) was dissolved in 30 mL of methanol. Sodium borohydride (0.76 g, 0.020 mol) in 6 mL of NaOH (0.2 M) was added dropwise to the solution cooled on ice. The reaction was allowed to continue for 1 h at room temperature. The black precipitate was removed by vacuum filtration and the methanol was removed under reduced pressure. The remaining aqueous suspension was diluted with 10 mL of sodium carbonate solution and then extracted with chloroform. The chloroform solution was dried over magnesium sulfate, and the chloroform was removed under reduced pressure. Yield: 2.0 g, 0.010 mol (50%). ^{1}H NMR ($CDCl_3$): CH_3, 2.42; CH_2O, 4.79; aromatic, 7.04–8.62.

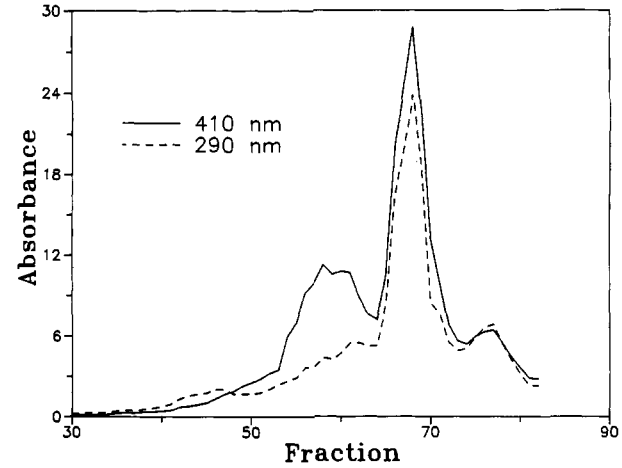

FIGURE 1: Purification of Ru-102-cyt *c*. The crude reaction mixture of Ru-ferricytochrome *c* (100 mg) was chromatographed on a 1.5 × 30 cm CM-52 (carboxymethyl)cellulose column with an exponential gradient from 100 to 400 mM sodium phosphate, pH 6.0. The fraction size was 1 mL. The absorbance was monitored at 410 and 286 nm.

(*C*) [*Ru*(*bpy*)$_2$(*4-hydroxymethyl-4′-methylbipyridine*)](*PF*$_6$)$_2$. $Ru(bpy)_2Cl_2$ (0.70 g, 0.0015 mol) was dissolved in 30 mL of water along with 4-hydroxymethyl-4′-methylbipyridine (0.65 g, 0.033 mol) and refluxed for 1 h. The color changed from black to bright red. The solution was vacuum-filtered and a concentrated solution of ammonium hexafluorophosphate was added at 4 °C to precipitate the product. The suspension was vacuum-filtered until nearly dry and then washed with ethyl ether. Yield: 1.48 g, 0.0020 mol (67%). ^{1}H NMR (CD_3CN): CH_3, 2.55; CH_2O, 4.82; aromatic, 7.2–8.56.

(*D*) [*Ru*(*bpy*)$_2$(*4-bromomethyl-4′-methylbipyridine*)](*PF*$_6$)$_2$. $[Ru(bpy)_2$(4-hydroxymethyl-4′-methylbipyridine)$](PF_6)_2$ (0.5 g) was refluxed for 3 h in 10 mL of HBr (48%) and 1 mL of H_2SO_4 (98%). After cooling, the product was precipitated by adding a concentrated solution of NH_4PF_6 until no further precipitation was observed. The suspension was filtered on a fritted funnel, washed extensively with ethyl ether, and dried under vacuum. The dry powder was stored in a desiccator at −90 °C. ^{1}H NMR (CD_3CN): CH_3, 2.55; CH_2Br, 4.68; aromatic, 7.2–8.64. The extinction coefficient was 13 500 M^{-1} cm^{-1} at 452 nm.

Preparation and Characterization of Yeast Cytochrome c Labeled with Ru(*bpy*)$_2$(*4-bromomethyl-4′-methylbipyridine*). Yeast cytochrome *c*, 1 mM in 1 mL of 50 mM Tris-HCl, pH 8.0, was treated with 1 mM dithiothreitol for 10 min to reduce any disulfide cross-linked dimer, and 5 mM $[Ru(bpy)_2$(4-bromomethyl-4′-methylbipyridine)$](PF_6)_2$ was added from a 100 mM stock solution in dry DMF. After 16 h at room temperature, the reaction mixture was passed through a Bio-Gel P-2 column (1.5 × 20 cm) equilibrated with 50 mM sodium phosphate, pH 6.0, to remove excess reagent. The cytochrome *c* derivative was purified by chromatography on a 1.5 × 30 cm Whatman CM-52 column eluted with an exponential gradient from 100 to 400 mM sodium phosphate, pH 6.0 (Figure 1). The UV/visible spectrum of the major peak was equal to the sum of the spectra of 1 equiv of $Ru(bpy)_2(dmbpy)^{2+}$ (ϵ_{452} = 13 500 M^{-1} cm^{-1}) and 1 equiv of native cytochrome *c* (Figure 2), indicating that this peak contained singly labeled $Ru(bpy)_2(dmbpy)$–cytochrome *c*. A small amount of native cytochrome *c* eluted earlier, while a small amount of labeled material eluted later. Peptide mapping was carried out essentially as described by Pan et al. (1988). An aliquot was dialyzed into 0.1 M Bicine, pH 8.0,

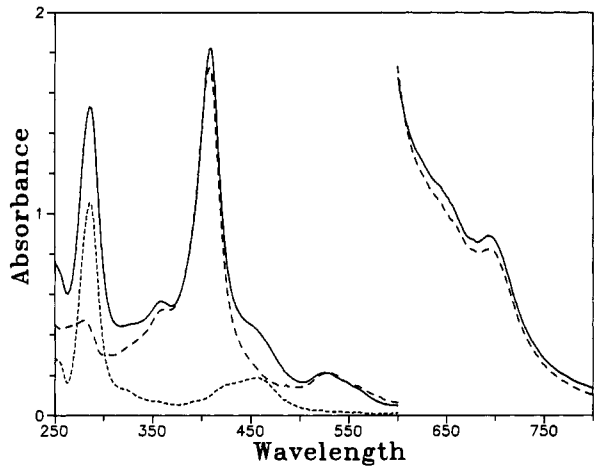

FIGURE 2: Visible absorption spectrum of purified Ru-102-ferricytochrome *c*. The UV/visible absorption spectrum of the derivative was recorded in 10 mM sodium phosphate, pH 7.0 (—). The concentration was 16 μM for the 250–600-nm range and 900 μM for the 600–800-nm range. Spectra of native yeast cytochrome c (---) and $Ru(bpy)_2(dmbpy)$ (---) are shown for comparison.

and 1% octyl glucoside at a concentration of 1 mg/mL and digested with two additions of 0.1 mg/mL TPCK-treated trypsin for 15 h at 37 °C. The tryptic digest was chromatographed on a Dynamax 300-Å reverse-phase HPLC column with a linear gradient from 0.01% trifluoroacetic acid to 100% methanol. The eluent was monitored at 210 and 290 nm by using two detectors in series. A single ruthenium-labeled peptide eluting at 17% methanol was observed in the 290-nm trace of the labeled cytochrome *c*. Amino acid sequencing indicated that this peptide was Ala_{101}-Ru-Cys_{102}-Asp_{103}, consistent with modification at Cys 102 (Dickerson, 1972). The redox potential of the heme group in Ru-102-cyt *c* was determined as described in Pan et al. (1988).

Transient Absorption Kinetics. Transient absorbance measurements were carried out by flash photolysis of 300-μL solutions contained in a 1-cm glass semimicrocuvette. The excitation light flash was provided by a Phase R Model DL1400 flashlamp-pumped dye laser using coumarin 450 to produce a 450-nm light pulse of <0.5-μs duration. The excitation beam was focused on the entire volume of the detection beam in the sample cuvette by a cylindrical lens. In some experiments, a xenon flash lamp with adjustable pulse width was used to excite the entire volume of the sample as described by Pan et al. (1990). The absorbance detection system is described in Pan et al. (1990). The absorbance transients were analyzed with the KINFIT kinetics program for single- and double-exponential decays supplied by On-Line Instrument Systems, Inc.

RESULTS

Preparation and Characterization of Yeast Ru-102-cyt c. The synthesis of $[Ru(bpy)_2(4\text{-bromomethyl-4'-methylbipyridine})](PF_6)_2$ described under Experimental Procedures utilizes conventional organic transformations. In the first step, refluxing 4,4'-dimethyl-2,2'-bipyridine with selenium(IV) oxide in 1,4-dioxane led to the clean oxidation of one of the two methyl groups to the aldehyde (Furue et al., 1986; Gosh & Spiro, 1981). The aldehyde was reduced to an alcohol with sodium borohydride and then complexed with $Ru(bpy)_2Cl_2$, and the OH was substituted with Br. The products isolated in each step were at least 95% pure. ^1H NMR of the products showed no extraneous resonances, and the changes in chemical shifts were consistent with the desired chemical transformations. Cyclic voltammetry of the final ruthenium product in CH_3CN showed only a single reversible oxidative wave with $E_{1/2}$ = 1.28 V vs a standard calomel electrode.

Scheme III

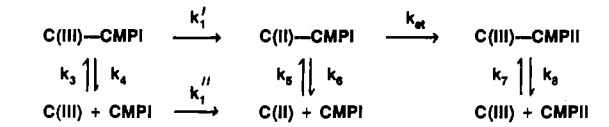

Yeast iso-1-cytochrome *c* contains a single sulfhydryl group at Cys 102 that is readily labeled by sulfhydryl-selective reagents (Montonaga et al., 1965; Saigo, 1986; Moench & Satterlee, 1989). $[Ru(bpy)_2(4\text{-bromomethyl-4'-methylbipyridine})](PF_6)_2$ was found to selectively label Cys 102 on iso-1-cytochrome *c*, as described under Experimental Procedures. Under the same conditions, the reagent did not label horse cytochrome *c*, which does not contain any free sulfhydryl groups. The reagent did label bovine serum albumin, which contains a free cysteine residue that is readily labeled by other cysteine reagents (Steinemann et al., 1978). HPLC peptide mapping demonstrated that the purified derivative was labeled exclusively at Cys 102. The UV/visible spectrum of the purified derivative was equal to the sum of the spectra of 1 equiv of $Ru(bpy)_2(dmbpy)^{2+}$ and 1 equiv of native yeast cytochrome *c* (Figure 2). The 695-nm band was unchanged in the derivative, indicating that the bond between the Met 80 sulfur atom and the heme iron was intact. The redox potential of the heme group in the derivative was found to be 260 ± 10 mV, the same as the value for native yeast cytochrome *c*. The derivative had a luminescence emission spectrum centered at 618 nm, with a luminescence decay rate of 5.2×10^6 s^{-1} (at 25 °C in air-saturated 0.1 M sodium phosphate, pH 7). By comparison, the luminescence decay rate of bovine serum albumin labeled with $Ru(bpy)_2(dmbpy)$ was 1.9×10^6 s^{-1}.

Photoinduced Electron Transfer from Ru-102-cyt c to Cytochrome c Peroxidase. Excitation of the Ru-102-cyt *c* derivative with a 450-nm laser pulse resulted in formation of Ru(II*), which rapidly transferred an electron to the heme group Fe(III) as shown in Scheme I. EDTA was used as a sacrificial electron donor, D, to reduce Ru(III) and prevent the back reaction k_2. The rate constant for reduction of Fe(III) was larger than the response rate of our detection system (10^5 s^{-1}), as was the rate of the reaction between EDTA and Ru(III). Flash photolysis of a solution containing Ru-102-cyt *c* and cytochrome *c* peroxidase compound I (CMPI) resulted in rapid photoreduction of the cytochrome *c* heme followed by electron transfer to CMPI (Figure 3A, Scheme III). The pseudo-first-order rate constant, k_{obs}, was 2400 ± 300 s^{-1} for a solution containing 5 μM Ru-102-cyt *c* and 5 μM CMPI in intermediate ionic strength buffer (5 mM sodium phosphate, pH 7, and 40 mM EDTA).

The product of the initial electron transfer step was characterized by monitoring the reaction at 420 nm. At this wavelength, the CMPI oxyferryl heme Fe(IV) to Fe(III) reaction has an extinction coefficient change of 31 mM^{-1} cm^{-1}, whereas the $R^{\bullet+}$ to R reaction has a Δε of nearly zero (Coulson et al., 1971; Ho et al., 1983). The $\Delta\epsilon_{420}$ for cytochrome *c* is 44 mM^{-1} cm^{-1}. The 420-nm transient showed no net absorbance change due to reduction of CMPI (Figure 3A), indicating that Ru-102-cyt *c* transferred an electron exclusively to the radical cation in CMPI according to reaction 1.

$$\text{cyt } c^{2+} + \text{CMPI(IV,R}^{\bullet+}) \rightarrow \text{cyt } c^{3+} + \text{CMPII(IV,R)} \quad (1)$$

$$\text{cyt } c^{2+} + \text{CMPII(IV,R)} \rightarrow \text{cyt } c^{3+} + \text{CcP(III,R)} \quad (2)$$

When the sample was subjected to additional flashes, the transients became biphasic and began to show a net decrease

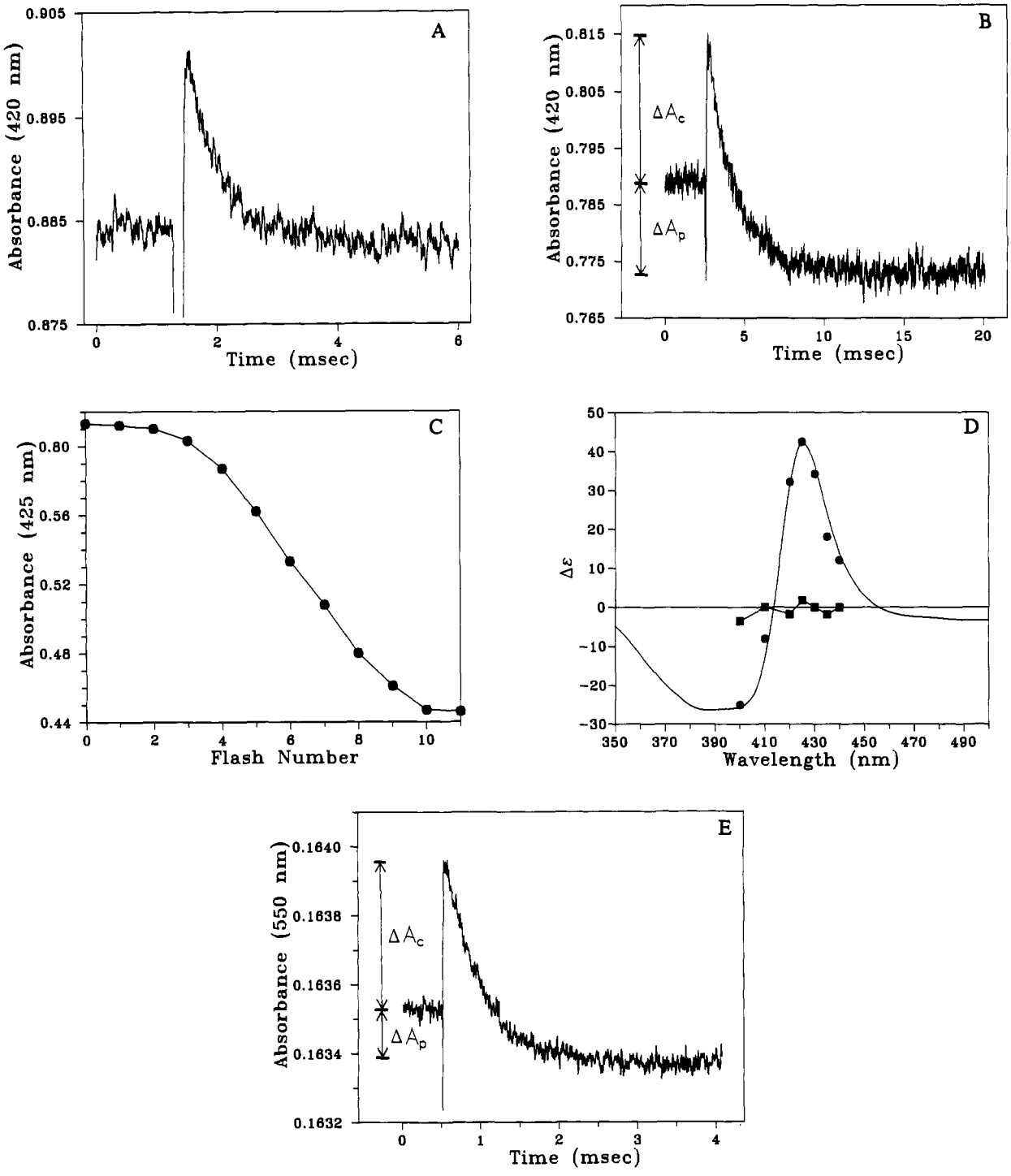

FIGURE 3: Photoinduced electron transfer from Ru-102-cyt *c* to cytochrome *c* peroxidase at intermediate ionic strength. All solutions contained 5 μM Ru-102-cyt *c* and 5 μM CMPI in 5 mM sodium phosphate, pH 7, and 40 mM EDTA. (A) 420-nm transient after a single xenon flash. (B) 420-nm transient of solution in (A) following the fifth xenon flash halfway through the titration from CMPI to CcP. (C) Flash titration of solution followed at 425 nm. The solution was subjected to a series of xenon flashes separated by 1 min each. The absorbance at 425 nm was measured 1 min after each flash. (D) Wavelength dependence of transient ΔA_p observed after the first flash (■) and after the fifth flash halfway through the titration (●). $\Delta\epsilon_p$ was calculated from the formula $\Delta\epsilon_p = \Delta A_p \Delta\epsilon_c / \Delta A_c$ mM^{-1} cm^{-1}, where $\Delta\epsilon_c = 44.3$ mM^{-1} cm^{-1} is the extinction coefficient change for cytochrome *c* at 420 nm and ΔA_c is the absorbance transient observed at 420 nm for photoreduction of cytochrome *c*. The solid line is ε(CMPI) − ε(CcP). (E) 550-nm transient for reaction between Ru-102-cyt *c* and CMPI after a single laser flash.

in absorbance (Figure 3B), indicating reduction of Fe(IV). A plot of a titration with light pulses (Figure 3C) had the same shape observed by Coulson et al. (1971) for a titration with ferrocyanide at high pH and is consistent with the reaction sequence (1) and (2). The titration was monitored at 425 nm where the maximum Δε for Fe(IV) − Fe(III) occurs.

The total absorbance change of the transient decay at any wavelength is $\Delta A = \Delta A_c + \Delta A_p$, where ΔA_c is due to the oxidation of ferrocytochrome *c* and ΔA_p is due to the reduction of CMPI. The value of ΔA_c was obtained from the increase in absorbance immediately after the flash, while ΔA_p was obtained from the difference in absorbance before the flash and at a long time after the flash (Figure 3B). The value of ΔA_p for the first transient was very small over the wavelength range 400–440 nm (Figures 3A,D), consistent with electron transfer to the radical. The wavelength dependence for the absorbance change ΔA_p, measured halfway through the titration (Figure 3D), was in good agreement with the absor-

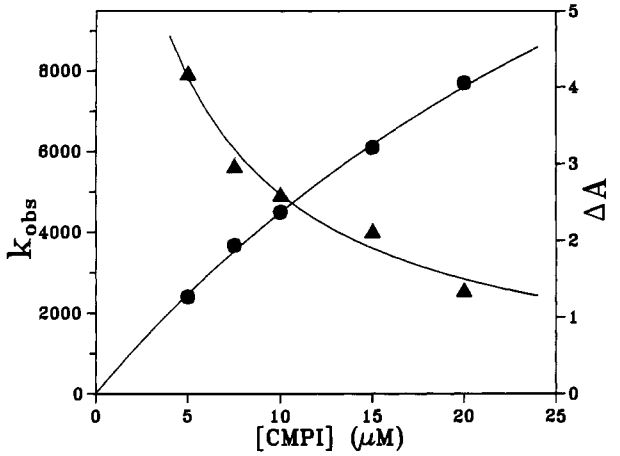

FIGURE 4: Concentration dependence of electron transfer from Ru-102-cyt *c* to cytochrome *c* peroxidase. A solution containing 5 μM Ru-102-cyt *c* and 5–20 μM CMPI in 40 mM EDTA and 5 mM sodium phosphate, pH 7, was excited with a single laser flash and the transient was detected at 550 nm. (▲) The amplitude of the transient, $\Delta A = 10^4(\Delta A_c + \Delta A_p)$, is plotted against the right axis. The solid line is the best fit to the binding equation. $\Delta A = \Delta A_0 [1 - (C + P + K_d - [(C + P + K_d)^2 - 4CP]^{0.5})/2C]$, where C is the total concentration of Ru-102-cyt *c*, P is the total concentration of CMPI, and $K_d = 4$ μM (Vitello and Erman, 1987). (●) The k_{obs} values for the transients are plotted against the left axis. The solid line is the best fit to eq 3 with $k_{et} = 25\,000$ s^{-1} and $k_5 = 4.8 \times 10^8$ M^{-1} s^{-1}.

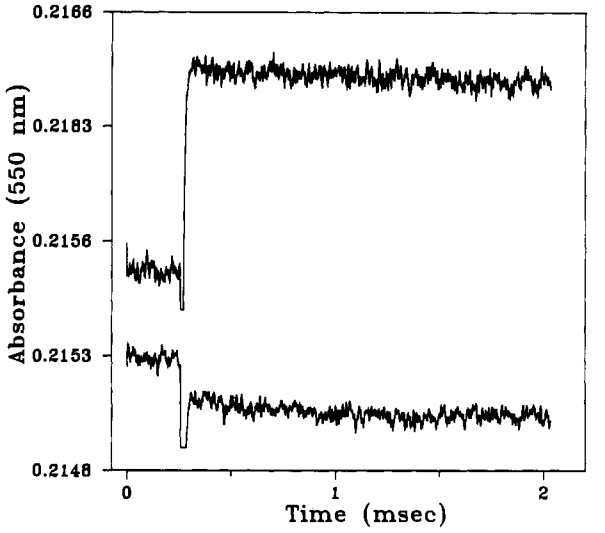

FIGURE 5: Photoinduced electron transfer from Ru-102-cyt *c* to cytochrome *c* peroxidase at low ionic strength. The solution contained 5 μM Ru-102-cyt *c* and 6 μM cytochrome *c* peroxidase in 5 mM EDTA and 5 mM sodium phosphate, pH 7.0. (Top) 550-nm transient for Ru-102 cyt *c* and CcP containing no hydrogen peroxide following a single laser flash. (Bottom) 550-nm transient for Ru-102-cyt *c* and CMPI after a single laser flash.

bance difference spectrum for CMPII(IV,R) – CcP(III,R) (Coulson et al., 1971; Ho et al., 1983). Reaction 2 could be observed without interference from reaction 1 at the cytochrome *c* isosbestic wavelength, 432 nm, and had a k_{obs} of 500 ± 50 s^{-1} under the conditions of Figure 3. A single sample could be subjected to at least two complete cycles of CMPI formation and flash titration back to CcP with the same rate constants and spectral properties at each stage of the titration. This indicates that there was no significant photolysis damage under the conditions used.

The kinetics for the initial reaction 1 were also monitored at 550 nm as illustrated in Figures 3E and 4. At this wavelength $\Delta\epsilon_p$ for the radical is 2 mM^{-1} cm^{-1} and $\Delta\epsilon_c$ for cytochrome *c* is 18.6 mM^{-1} cm^{-1} (Coulson et al., 1971; Ho et al., 1983). The amplitude of the transient decay, $\Delta A_c + \Delta A_p$, decreased significantly as the CMPI concentration increased, while the rate constant increased nearly linearly. The decrease in amplitude was due entirely to a decrease in ΔA_c. ΔA_p remained constant, indicating that the amount of CMPI reduced per flash was unchanged as the total concentration of CMPI increased. This behavior can be rationalized with Scheme III if the Ru-102-cyt *c* that is bound to CMPI at the time of the flash transfers an electron so rapidly to the radical cation that the reaction is not resolved in the dead time of the instrument (see below). The observed transient decay is thus due to the reaction of Ru-102-cyt *c* that is free in solution at the time of the flash. The decrease in amplitude of the transient decay, therefore, indicates formation of a complex between Ru-102-cyt *c* and CMPI prior to excitation. A dissociation constant $K_d = k_4/k_3$ was estimated to be 4 ± 2 μM, as shown in Figure 4.

Immediately following the laser pulse, the kinetics of solution Ru-102-cyt *c* can be described by rate constants k_5, k_6, and k_{et} of Scheme III. The concentration dependence of k_{obs} for such a system has been described by Strickland et al. (1975):

$$k_{obs} = k_5 k_{et}[\text{CMPI}]/(k_5[\text{CMPI}] + k_6 + k_{et}) \quad (3)$$

Since the dependence of k_{obs} on [CMPI] was nearly linear (Figure 4), only a lower limit for k_{et} of 25 000 s^{-1} could be obtained. k_5 was estimated to be (4.8 ± 0.5) × 10^8 M^{-1} s^{-1} from the linear region of the curve at low CMPI concentrations. In this analysis it was assumed that k_6 was small compared to k_{et}, since if $k_6 > k_{et}$ there would be no difference in the kinetics of bound and free Ru-102-cyt *c* and hence no decrease in the amplitude of the transient.

The very rapid electron transfer rate for the bound complex became even more apparent at low ionic strength, where a tight complex is expected to be formed. One equivalent (5 μM) of CMPI was sufficient to completely eliminate the positive ΔA_c due to photoreduction of 5 μM Ru-102-cyt *c* and resulted in an immediate decrease in the 550-nm absorbance by an amount equal to ΔA_p (Figure 5). The decrease in absorbance was complete within the response time of the detection system, which was limited by light scattering. Taking this into account, k_{obs} was estimated to be larger than 50 000 s^{-1}. Increasing the concentration of CMPI above 1 equiv had no further effect on the transient, indicating that the dissociation constant K_d was less than 1 μM. No absorbance change at all was observed at 420 nm, consistent with electron transfer to the radical site in CMPI. As the sample was titrated with additional flashes, a slow transient began to appear at both 420 and 550 nm that had the correct wavelength dependence for reaction 2. The rate constant for this reaction was 250 ± 50 s^{-1} in 5 mM EDTA and 5 mM phosphate, pH 7, and remained constant when the concentration of cytochrome *c* peroxidase was increased. This intracomplex rate constant was highly dependent on ionic strength, increasing to 1000 ± 200 s^{-1} in 10 mM EDTA and 5 mM sodium phosphate, independent of the concentration of cytochrome *c* peroxidase. At higher ionic strengths this reaction became second order as described above for reaction 1. Sodium phosphate and NaCl affected the kinetics in a fashion similar to that of EDTA, increasing the rate of reaction 2 until it became second order and then decreasing the second-order rate constants for both reactions at higher ionic strengths. The second-order rate constant for reaction 1 decreased from (1.3 ± 0.2) × 10^{-8} M^{-1} s^{-1} in 200 mM NaCl to (1.6 ± 0.2) × 10^7 M^{-1} s^{-1} in 500 mM NaCl.

The flavin flash photolysis technique developed by Hazzard et al. (1987, 1988a–c) was used to compare the electron

transfer kinetics of native and Ru-102-cyt c under identical conditions. Low-intensity light flashes were used to photoreduce about 0.1 μM lumiflavin, which then reduced cytochrome c. At high ionic strength (100 mM sodium phosphate, pH 7, 25 mM EDTA, and 50 μM lumiflavin) k_{obs} for native iso-1-cytochrome c increased linearly with [CMPI] over the range 0.5–5 μM and exhibited a second-order rate constant of $(6.7 \pm 0.7) \times 10^7$ M^{-1} s^{-1}. This is essentially the same as that observed by Hazzard et al. (1988a) under these conditions. The second-order rate constant for Ru-102-cyt c was $(7.5 \pm 0.7) \times 10^7$ M^{-1} s^{-1} under these conditions, measured by either lumiflavin excitation or ruthenium excitation. (The low flash intensity used for lumiflavin excitation does not produce a significant amount of ruthenium-based products.) These results indicate that Ru-102-cyt c has the same kinetic properties as native cytochrome c at high ionic strength. However, at low ionic strength (3 mM sodium phosphate and 0.5 mM EDTA, pH 7) no detectable reduction of Ru-102-cyt c by photoreduced lumiflavin was observed at 550 nm in the presence of excess CMPI. In contrast, native iso-1-cytochrome c was rapidly reduced by photoreduced lumiflavin under the same conditions, and the intracomplex reaction with CMPI could be measured as described by Hazzard et al. (1988a).

Discussion

$Ru(bpy)_2$(4-bromomethyl-4′-methylbipyridine)$^{2+}$ was found to efficiently label the single sulfhydryl group at Cys-102 on the back side of yeast iso-1-cytochrome c. This reagent thus provides a simple method to selectively attach the $Ru(bpy)_2$(dmbpy) group to proteins containing a free sulfhydryl. Ru-102-cyt c has the same heme redox potential and visible spectrum as native cytochrome c, including the 695-nm band associated with the bond between the Met 80 sulfur atom and the heme iron. The derivative is thus likely to have nearly the same conformation in the heme crevice region as native cytochrome c (Pearce et al., 1989; Louie et al., 1988). However, the X-ray crystal structure of native iso-1-cytochrome c revealed that the Cys-102 side chain is buried within the COOH-terminal helix (Louie et al., 1988), and thus modification of this residue must involve some degree of local unfolding. In fact, high-field NMR studies have shown that modification of Cys-102 with thionitrobenzoate resulted in small chemical shift changes for protons throughout the molecule (Moench & Satterlee, 1989). These changes are nearly identical with those observed in the dimer form of the enzyme linked by a disulfide bond between the two Cys-102 residues. Neither dimerization nor chemical modification of Cys-102 alters the enzymatic activity of iso-1-cytochrome c, but they do affect its stability toward denaturation and ligand binding (Saigo, 1986; Montonaga et al., 1965; Bryant et al., 1985). NMR studies (500 MHz) of $Ru(bpy)_2$(dmbpy)–cytochrome c are currently in progress in our laboratory and will be reported elsewhere. Preliminary results have shown that the hyperfine-shifted resonances in the oxidized protein have chemical shifts essentially identical with those reported by Moench and Satterlee (1989) for the dimeric protein and the protein modified with thionitrobenzoate. The second-order rate constant for the reaction between Ru-102-cyt c and cytochrome c peroxidase CMPI was the same as that of native iso-1-cytochrome c at high ionic strength, providing evidence that the activity of the derivative is not impaired.

An important question regarding the mechanism of cytochrome c peroxidase is whether cytochrome c initially transfers an electron to the free radical site or to the heme Fe(IV) in CMPI. The kinetic studies reported here provide definitive evidence that at pH 7 Ru-102-cyt c first transfers an electron to the radical site in CMPI and subsequently to the heme Fe(IV) site in CMPII, according to eqs 1 and 2. This order for electron transfer was obeyed at all ionic strengths and is the same observed during equilibrium titration with ferrocyanide or ferrocytochrome c at pH values of 7 and above (Coulson et al., 1971). In contrast, Summers and Erman (1988) reported that native horse cytochrome c reduced only the Fe(IV) site of CMPI in stopped-flow experiments at low ionic strength. Since the radical site was not reduced directly, they proposed a mechanism in which the radical form of CMPII was converted to the oxyferryl heme form before reaction with cytochrome c could occur.

The reaction between photoreduced Ru-102-cyt c and cytochrome c peroxidase was second order at ionic strengths down to about 200 mM, with a rate constant that increased with decreasing ionic strength. The kinetics departed from second order in 40 mM EDTA, where the effects of complex formation were observed (Figure 4). The dissociation constant K_d for Ru-102-cyt c binding to CMPI was estimated to be 4 ± 2 μM in this buffer, which compares favorably to $K_d = 2$ μM for native yeast iso-2-cytochrome c binding to CcP in 0.2 M Tris/cacodylate buffer at pH 6 (Kang et al., 1977). The K_d for native iso-1-cytochrome c binding to porphyrin CcP has been estimated to be 13 μM in 100 mM potassium phosphate, pH 7 (Leonard & Yonetani, 1974). The association rate constant k_5 was estimated to be $(4.8 \pm 0.5) \times 10^8$ M^{-1} s^{-1} for Ru-102-cyt c in 40 mM EDTA. This is in good agreement with the association rate constant of 5.6×10^8 M^{-1} s^{-1} measured for native yeast iso-1-cytochrome c in 0.2 M sodium acetate, pH 6.0 (Yonetani & Ray, 1966). The dissociation rate constant for the complex between horse ferricytochrome c and CcP has been estimated to be larger than 1100 s^{-1} in low ionic strength buffer (Satterlee et al., 1987). Although the dissociation rate constant has not been reported for native iso-1-cytochrome c, it is likely to be smaller than that for horse cytochrome c because of the much smaller K_d value. Our conclusion that k_6 for Ru-102-cyt c is smaller than k_{et}, therefore, appears reasonable.

At low ionic strength (5 mM sodium phosphate and 5 mM EDTA, pH 7), 1 equiv of CMPI completely eliminated the positive ΔA_c associated with photoreduction of Ru-102-cyt c and resulted in a rapid decrease in the 550-nm absorbance within the response time of the detector. The rate constant for intracomplex electron transfer from the heme group of Ru-102-cyt c to the radical in CMPI was estimated to be greater than 50 000 s^{-1}. The rate constant k_1' for electron transfer from ruthenium group to the heme group in Ru-102-cyt c was also greater than 50 000 s^{-1}. The dissociation constant K_d was estimated to be less than 1 μM, which compares favorably to $K_d < 0.01$ μM for native yeast iso-2-cytochrome c in 10 mM Tris/chloride, pH 6 (Kang et al., 1977). An alternative mechanism for the kinetics at low ionic strength is that Ru-102-cyt c could bind to the peroxidase with the back surface Ru-Cys 102 located near the reaction site such that it could directly reduce the radical in CMPI rather than the heme group in Ru-102-cyt c. However, this binding orientation would leave the heme crevice on cytochrome c exposed, whereas the heme in Ru-102-cyt c was found to be protected from reduction by photoreduced lumiflavin when bound to CMPI. In addition, the kinetic data for solution Ru-102-cyt c at higher ionic strength (Figure 4) provide direct evidence that the rate of electron transfer from the Ru-102-cyt c heme to the radical is greater than 25 000 s^{-1}.

The rate constant for the reaction between cytochrome c and the oxyferryl heme Fe(IV) site in CMPII was much

smaller than that for reduction of the radical site in CMPI at all ionic strengths. This could be due to a higher reorganization energy for the oxyferryl heme Fe(IV) compared to the radical or due to poorer electronic coupling. The intracomplex rate constant for reduction of Fe(IV) increased from 250 ± 50 s^{-1} in 5 mM sodium phosphate and 5 mM EDTA to 1000 ± 200 s^{-1} in 5 mM sodium phosphate and 10 mM EDTA, suggesting that a more favorable orientation for rapid electron transfer was achieved at higher ionic strength. A similar effect was observed for the reaction between native iso-1-cytochrome *c* and CMPI, where the intracomplex rate constant increased from 250 s^{-1} at 8 mM ionic strength to 1460 s^{-1} at 260 mM ionic strength (Hazzard et al., 1988a).

Evidence for the existence of multiple conformational forms of the cytochrome *c*–cytochrome *c* peroxidase complex has been obtained by a number of techniques, including X-ray crystallography (Poulos et al., 1987), Brownian dynamics simulations (Northrup et al., 1987, 1988), and electron transfer studies involving zinc–cytochrome *c* peroxidase (Nocek et al., 1990; Wallin et al., 1991). Everest et al. (1991) have recently reported three kinetic phases for electron transfer from yeast iso-1-ferrocytochrome *c* to the zinc porphyrin cation of zinc–CcP, with rate constants of 4900 s^{-1}, 27 s^{-1}, and 3 s^{-1}. We have observed biphasic kinetics for the intracomplex reactions between the horse $Ru(bpy)_2(dcbpy)$–cytochrome *c* derivatives and the radical site in CMPI, with fast-phase rate constants ranging from 6000 s^{-1} to 47 000 s^{-1} (Hahm et al., 1991). Since the reaction between Ru-102-cyt *c* and the radical site in CMPI was too fast to measure at low ionic strength, the possibility of multiple kinetic phases could not be addressed. The kinetic traces for the reaction between Ru-102-cyt *c* and the Fe(IV) site in CMPII were adequately fit by single exponentials, but because of signal-to-noise limitations it would not have been possible to resolve a second phase with an amplitude of 10% or less, particularly if the rate constant was not greatly different from that of the major phase. Thus, no definitive conclusions about the existence of multiple binding forms can be made from this study.

The binding orientation of Ru-102-cyt *c*, however, appears to be quite different from that of native iso-1-cytochrome *c*, since complex formation with CMPI protected its heme group from reduction by lumiflavin semiquinone. The heme group of native iso-1-cytochrome *c* complexed to CMPI is highly accessible to lumiflavin semiquinone (Hazzard et al., 1988a), which may explain the slow rate of intracomplex electron transfer in this system. As mentioned above, preliminary NMR studies have suggested that the structure of Ru-102-cyt *c* is similar to that of dimeric iso-1-cytochrome *c* and different from that of monomeric iso-1-cytochrome *c*. Moench and Satterlee (1989) have suggested that modification of Cys-102 by dimerization might play a regulatory role in the physiological function of iso-1-cytochrome *c*. Thus, the very large intracomplex electron transfer rate observed for the Ru-102-cyt *c* derivative might have greater significance than just being a serendipitous alteration of the binding orientation.

References

Bryant, C., Strottmann, J. B., & Stellwagen, E. (1985) *Biochemistry 24*, 3459–3464.

Coulson, A. F. W., Erman, J. E., & Yonetani, T. (1971) *J. Biol. Chem. 246*, 917–924.

Dickerson, R. E. (1972) *Sci. Am. 226*, 58–72.

Durham, B., Pan, L. P., Long, J., & Millett, F. (1989) *Biochemistry 28*, 8659–8665.

Edwards, S. L., Xuong, N. H., Hamlin, R. C., & Kraut, J. (1987) *Biochemistry 26*, 1503–1511.

Everest, A. M., Wallin, S. A., Stemp, E. D. A., Nocek, J. M., Mauk, A. G., & Hoffman, B. M. (1991) *J. Am. Chem. Soc. 113*, 4337–4338.

Finzel, B. C., Poulos, T. L., & Kraut, J. (1984) *J. Biol. Chem. 259*, 13027–13036.

Furue, M., Kuroda, N., & Nozakura, S. (1986) *Chem. Lett.*, 1209–1212.

Gosh, P. K., & Spiro, T. G. (1981) *J. Electrochem. Soc. 128*, 1281–1287.

Hahm, S., Durham, B., & Millett, F. (1991) *Biochemistry* (submitted for publication).

Hazzard, J. T., Poulos, T., & Tollin, G. (1987) *Biochemistry 26*, 2836–2848.

Hazzard, J. T., McLendon, G., Cusanovich, M. A., & Tollin, G. (1988a) *Biochem. Biophys. Res. Commun. 151*, 429–434.

Hazzard, J. T., Moench, S. J., Erman, J. E., Satterlee, J. D., & Tollin, G. (1988b) *Biochemistry 27*, 2002–2008.

Hazzard, J. T., McLendon, G., Cusanovich, M. A., Das, G., Sherman, F., & Tollin, G. (1988c) *Biochemistry 27*, 4445–4451.

Ho, P. S., Hoffman, B. M., Kang, C. H., & Margoliash, E. (1983) *J. Biol. Chem. 258*, 4356–4363.

Kang, C. H., Ferguson-Miller, S., & Margoliash, E. (1977) *J. Biol. Chem. 252*, 919–926.

Kim, K. L., Kang, D. S., Vitello, L. B., & Erman, J. E. (1990) *Biochemistry 29*, 9150–9159.

Leonard, J. J., & Yonetani, T. (1974) *Biochemistry 13*, 1465–1468.

Louie, G. B., Pielak, G. J., Smith, M., & Brayer, G. D. (1988) *Biochemistry 27*, 7870–7876.

Mauro, J. M., Fishel, L. A., Hazzard, J. T., Meyer, T. E., Tollin, G., Cusanovich, M. A., & Kraut, J. (1988) *Biochemistry 27*, 6243–6256.

Moench, S. J., & Satterlee, J. D. (1989) *J. Biol. Chem. 264*, 9923–9931.

Montonaga, M., Katano, H., & Nakanishi, K. (1965) *J. Biochem. (Tokyo) 57*, 29–33.

Nocek, J. M., Liang, N., Wallin, S. A., Mauk, A. G., & Hoffman, B. M. (1990) *J. Am. Chem. Soc. 112*, 1623–1625.

Northrup, S. H., Boles, J. O., & Reynolds, J. C. L. (1987) *J. Phys. Chem. 91*, 5991–5998.

Northrup, S. H., Boles, J. O., & Reynolds, J. C. L. (1988) *Science 241*, 67–70.

Pan, L. P., Durham, B., Wolinska, J., & Millett, F. (1988) *Biochemistry 27*, 7180–7184.

Pan, L. P., Frame, M., Durham, B., Davis, D., & Millett, F. (1990) *Biochemistry 29*, 3231–3236.

Pearce, L. L., Gartner, A. L., Smith, M., & Mauk, A. G. (1989) *Biochemistry 28*, 3152–3156.

Poulos, T. L., & Kraut, J. (1980) *J. Biol. Chem. 255*, 10322–10330.

Poulos, T. L., Sheriff, S., & Howard, A. J. (1987) *J. Biol. Chem. 262*, 13881–13884.

Saigo, S. (1986) *J. Biochem. (Tokyo) 100*, 157–165.

Sivaraja, M., Goodin, D. B., Smith, M., & Hoffman, B. M. (1989) *Science 245*, 738–740.

Smith, M. B., & Millett, F. (1980) *Biochim. Biophys. Acta 626*, 64–72.

Steinemann, A., Bietenhader, J., & Dockter, M. (1978) *Anal. Biochem. 86*, 303–309.

Strickland, S., Palmer, G., & Massey, V. (1975) *J. Biol. Chem. 250*, 4048–4052.

Summers, F. E., & Erman, J. E. (1988) *J. Biol. Chem. 263*, 14267–14275.
Wallin, S. A., Stemp, E. D. A., Everest, A. M., Nocek, J. M., Netzel, T. L., & Hoffman, B. M. (1991) *J. Am. Chem. Soc. 113*, 1842–1844.
Wang, J., Mauro, J. M., Edwards, S. L., Oatley, S. J., Fishel, L. A., Ashford, V. A., Xuong, N. H., & Kraut, J. (1990) *Biochemistry 29*, 7160–7173.
Yonetani, T., & Ray, G. S. (1966) *J. Biol. Chem. 241*, 700–706.

Reexamination of the Role of Asp^{20} in Catalysis by Bacteriophage T4 Lysozyme†

Larry W. Hardy* and Anthony R. Poteete
Department of Molecular Genetics and Microbiology, University of Massachusetts, Worcester, Massachusetts 01655
Received September 4, 1990; Revised Manuscript Received July 18, 1991

ABSTRACT: Replacement of Asp^{20} in T4 lysozyme by Cys produces a variant with (1) nearly wild-type specific activity, (2) a newly acquired sensitivity to thiol-modifying reagents, and (3) a pH–activity profile that is very similar to that of the wild-type enzyme. These results indicate that the residue at position 20 has a significant nucleophilic function rather than merely an electrostatic role. The intermediate in catalysis by lysozyme is probably a covalent glycosyl-enzyme instead of the ion pair originally proposed.

Lysozyme provides an essential function in the life cycle of the phage—the destruction of the bacterial cell wall necessary for the release of progeny phage particles. The enzyme catalyzes the hydrolysis of the β-1,4 glycosidic linkages of the alternating copolymer of *N*-acetylmuramic acid and *N*-acetylglucosamine in bacterial peptidoglycan. Little has been published on the mechanism of catalysis by T4 lysozyme, in contrast to the abundant literature on the catalytic mechanism of hen egg white (HEW) lysozyme. HEW lysozyme is the first enzyme whose atomic structure was visualized by X-ray diffraction analysis (Blake et al., 1965). The three-dimensional structure of T4 lysozyme is also known (Remington et al., 1978; Weaver & Matthews, 1987). The remarkable similarity of the geometries of the active sites of HEW and T4 lysozymes (Anderson et al., 1981; Matthews et al., 1981) strongly suggests that the two enzymes catalyze hydrolysis of glycosides via a similar or common mechanism. Inspection of the structure of HEW lysozyme in complex with substrate analogues led directly to a detailed proposal for its mechanism (Blake et al., 1967; Vernon, 1967), depicted in Figure 1A, which is presented in many textbooks of biochemistry to exemplify principles of enzymatic catalysis. The first step of that mechanism is protonation by a Glu residue (Glu^{35} in HEW or Glu^{11} in T4) of the oxygen (O_4'), which in the substrate links C_1 of the incipient reducing sugar and C_4' of the departing glycosyl moiety. The next step, bond cleavage between the protonated O_4' and C_1, is assisted by participation of the ring oxygen (O_5), yielding an endocyclic oxocarbonium ion intermediate. The glycosyl carbonium ion is thought to be stabilized by electrostatic interaction with the carboxylate side group of an Asp residue (Asp^{52} in HEW or Asp^{20} in T4). Finally, the proposed carbonium ion intermediate reacts with water (or some other acceptor) to complete the reaction. Covalent catalysis by the carboxylate of the active-site Asp (Figure 1B) was considered but regarded as unlikely in the original formulation of the mechanism (Blake et al., 1967; Vernon, 1967). Many subsequent assessments have concurred with this view, but no available evidence conclusively demonstrated or ruled out the existence of either of the intermediates shown in Figure 1 (Kirby, 1987).

While carrying out systematic studies of the effects of single amino acid substitutions on the function of T4 lysozyme, we made the initially surprising observation that substitution of Asp^{20} with Cys produced a functional enzyme. Comparison of the properties of the purified mutant T4 lysozyme (hereafter designated D20C) with those of the wild-type protein, described in this paper, provides strong evidence against a merely electrostatic role for the residue at position 20 in this enzyme and instead implies that catalysis occurs with substantial covalent bond formation between the carboxylate of the active-site Asp and C_1 of the glycosyl-enzyme intermediate.

Experimental Procedures

Phage Methods. Hybrid P22 phages bearing mutant and wild-type alleles of the T4 lysozyme gene (*e*) were constructed by crosses of P22 *Kn321 sieA44 m44* with plasmids, as previously described (Rennell & Poteete, 1989; see Figure 2). Those regions of DNA which were single-stranded in the gapped duplex DNA (gdDNA)[1] were sequenced in the hybrid phages as described (Rennell & Poteete, 1989) to ensure that only the desired mutations were present. *Salmonella typhimurium* and *Escherichia coli* strains, phage, media, and culture methods were described by Rennell and Poteete (1989).

Plasmid Construction. Plasmid pTP400 contains (in order) the following sequences: the segment of pZ152 (Zagursky & Berman, 1983) bearing the plasmid replication origin, filamentous phage IG sequence, and *bla* gene, bounded by *Pvu*II (converted to *Bam*HI in pTP400) and *Eco*RI (converted to *Sal*I) sites; P22 DNA from the *Rsa*I site in gene *13* to the proximal *Hin*fI site in gene *19* (244 bp; Rennell & Poteete, 1985); a synthetic linker, formed by two oligomers (5′-AATCTAAGC-3′ and 5′-TAAGCTTAG-3′); T4 DNA from

† This work was supported by a grant from NIH (AI18234 to A.R.P.)
* To whom correspondence should be addressed at the Department of Pharmacology, University of Massachusetts Medical Center, 55 Lake Ave. N., Worcester, MA 01655.

[1] Abbreviations: dNTP, 2′-deoxynucleoside triphosphates; EDTA, disodium ethylenediaminetetraacetate; gdDNA, gapped duplex DNA; Tris, tris(hydroxymethyl)aminomethane.

0006-2960/91/0430-9457$02.50/0